

A Geometric Approach to Inelastic Collapse*

Bernard Chazelle¹, Kritkorn Karntikoon², and Yufei Zheng³

1 Department of Computer Science, Princeton University
chazelle@cs.princeton.edu

2 Department of Computer Science, Princeton University
kritkorn@cs.princeton.edu

3 Department of Computer Science, Princeton University
yufei@cs.princeton.edu

1 Abstract

2 We show in this note how to interpret logarithmic spiral tilings as one-dimensional particle
3 systems undergoing inelastic collapse. By deforming the spirals appropriately, we can simulate
4 collisions among particles with distinct or varying coefficients of restitution. Our geometric
5 constructions provide a strikingly simple illustration of a widely studied phenomenon in the
6 physics of dissipative gases: the collapse of inelastic particles.

Lines 154

7 1 Introduction

8 Collisions in a granular gas preserve momentum but not kinetic energy. Interactions are
9 dissipative, with the velocities of two colliding particles governed by a stochastic matrix
10 $\begin{pmatrix} p & q \\ q & p \end{pmatrix}$, for $p \leq 1/2$. When the coefficient of restitution, defined as $r = 1 - 2p$, is less than
11 1, the collisions are inelastic and the particles may collapse to a single point in a finite
12 amount of time: this intriguing phenomenon of *inelastic collapse* was first investigated in
13 one dimension by Bernu & Mazighi [2] and McNamara & Young [6]. Further studies and
14 extensions to a larger number n of particles were given in [1, 2, 3, 4, 5, 6, 7, 8]. In the case
15 $n = 3$, inelastic collapse requires $r < 7 - 4\sqrt{3}$ [4, 6, 7], while in general the requirement is that
16 $n \gtrsim 2(\ln 2)/(1 - r)$. Matching constructions for large n exist but entail intricate eigenvalue
17 estimates [1, 2]. We rederive these bounds by simple geometric means, and we also extend
18 them to other types of collisions. Our particle systems are derived from one-dimensional
19 projections of spiral tilings of a disk (see §2). Using different spirals allows the presence
20 of particles with different coefficients of restitution (see §3). The notable feature of our
21 arguments is to be entirely geometric.

22 2 The Inelastic Collapse of Identical Particles

23 We describe the dynamics of n identical particles moving towards the center of a disk and
24 colliding along the way. The one-dimensional system is derived by projection to a line. We
25 begin with the geometry of the system, which is a quadrilateral tiling of the complex unit
26 disk by logarithmic spirals.

27 2.1 Spiral tilings

28 We describe the dynamics of n identical particles moving towards the center of a disk and
29 colliding along the way. The one-dimensional system is derived by projection to a line. We

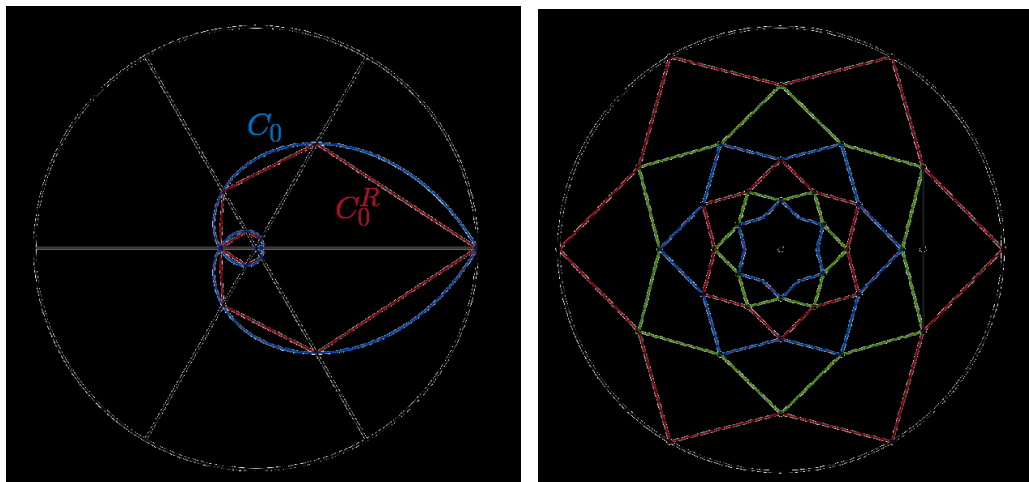
* This work was supported in part by NSF grant CCF-2006125.

37th European Workshop on Computational Geometry, St. Petersburg, Russia, April 7–9, 2021.
This is an extended abstract of a presentation given at EuroCG'21. It has been made public for the benefit of the
community and should be considered a preprint rather than a formally reviewed paper. Thus, this work is expected
to appear eventually in more final form at a conference with formal proceedings and/or in a journal.

30 begin with the geometry of the system, which is a quadrilateral tiling of the complex unit
31 disk by logarithmic spirals.

32 2.2 Spiral tilings

33 Fix $0 < \lambda_o < 1$ and let $\mathcal{C}_\alpha = \{ \lambda_o^{|\varphi-\alpha|} e^{i\varphi} \mid \varphi \in \mathbb{R} \}$. The curve \mathcal{C}_α consists of two logarithmic
34 spirals running clockwise and counterclockwise from the point $e^{i\alpha}$. The family $\{\mathcal{C}_\alpha\}_{0 \leq \alpha < 2\pi}$
35 forms two foliations of the unit complex disk \mathcal{D} (minus the origin). Whereas no pair of
36 spirals going in the same direction meet, the other pairs intersect infinitely often along the
37 diameter bisecting their starting points. Fix an integer $n > 2$ and write $\theta = \pi/n$. We rectify
38 the spiral \mathcal{C}_α by creating the vertices $\lambda_o^{k\theta-\alpha} e^{ik\theta}$ for all $k \in \mathbb{Z}$; then we join consecutive pairs
39 by straightline segments, which produces the polygonal spiral \mathcal{C}_α^R in Figure 1(i).



40 ■ **Figure 1** (i) The spirals \mathcal{C}_α and \mathcal{C}_α^R , for $\alpha = 0$ and $\theta = \pi/3$; (ii) an (n, λ) -tiling for a system of
41 $2n = 12$ colliding particles.

42 The collection of polygonal curves $\{\mathcal{C}_{2j\theta}^R \mid 0 \leq j < n\}$ forms an infinite sequence of nested
43 concentric similar $2n$ -gons $P_k := \lambda e^{i\theta} P_{k-1}$, where $\lambda = \lambda_o^\theta$ and P_0 is the outer “star” shown in
44 Figure 1(ii): its vertices $e^{il\theta} \lambda^{(1-(-1)^l)/2}$ run in counterclockwise order ($0 \leq l < 2n$). To ensure
45 that the shape is indeed a star, every other vertex of P_0 needs to be reflex, which requires
46 that $\lambda < \cos \theta$. This partitions the polygon P_0 into an infinite collection of similar convex
47 quadrilaterals, which forms an (n, λ) -tiling. We define the *fundamental ratio* $\rho := ae/ac$ of
48 the (n, λ) -tiling and justify its name by noting that it is independent of the polygon P_k used
49 to define it. Referring to Figure 1(ii), we observe that $ac = 1 - \lambda \cos \theta$ and $ae = \lambda \cos \theta - \lambda^2$
50 and that, for any $0 < \lambda < \cos \theta$,

$$51 \quad \rho = \frac{\lambda(\cos \theta - \lambda)}{1 - \lambda \cos \theta} \quad \text{and} \quad 0 < \rho < 1. \quad (1)$$

52 2.3 Particles traveling in a disk

53 Place two particles at each one of the n outer vertices of P_0 and set them in motion along
54 the two incident edges with a speed equal to bc . We show below that the particles will
55 zigzag toward the center (as in the trajectory c, b, e, f, g, \dots) provided that the coefficient of
56 restitution r is equal to $\rho < 1$, where $r = 1 - 2\rho$; recall that, whenever two particles with

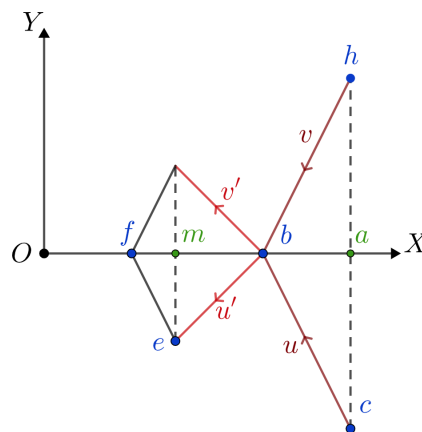
57 velocities $u, v \in \mathbb{C}$ collide, they bounce away from each other and update their velocities as
 58 follows:

$$59 \quad \begin{pmatrix} u \\ v \end{pmatrix} \leftarrow \begin{pmatrix} p & q \\ q & p \end{pmatrix} \begin{pmatrix} u \\ v \end{pmatrix};$$

60 where $0 < p < q < 1$ and $p + q = 1$.

61 ► **Lemma 2.1.** *The $2n$ particles travel along the edges of the tiling through pairwise collisions
 62 if and only if the fundamental ratio ρ is equal to the coefficient of restitution r . If each
 63 particle spends one unit of time on the boundary ∂P_0 , then it travels on ∂P_k for a duration
 64 of δ^k , where $\delta = \lambda^2/\rho$. The total travel time is bounded if and only if $\lambda < \frac{1}{\cos \theta} - \tan \theta$, in
 65 which case it is equal to $1/(1 - \delta)$.*

66 **Proof.** For convenience, we tilt the tiling by θ to put b and f on the X -axis (Figure 2). Two
 67 particles travel from c and h to b with velocity u and v respectively. The first one bounces
 68 at b and proceeds with velocity $u' = pu + qv$. Since $u_x = v_x$ and $u_y = -v_y$, we have $u'_x = u_x$
 69 and $u'_y = -ru_y$; therefore $|\text{slope}(u')| = r|\text{slope}(u)|$. By similarity, bc and ef are parallel; hence
 70 $|\text{slope}(u')| = r|\text{slope}(ef)|$. The consistency of the particle collision with the tiling means that
 71 u' should be parallel to the segment be . The condition thus becomes $|\text{slope}(be)| = r|\text{slope}(ef)|$;
 72 hence $r = mf/mc = \rho$.



73 ■ **Figure 2** How colliding particles follow the edges of the (n, λ) -tiling. The coefficient of restitution
 74 must be equal to the ratio $\rho = mf/mc$.

75 If the particle travels from c to b in one unit of time, then $u_y = ac$ and $u'_y = -ru_y = -rac$.
 76 It follows that the time δ for the particle to bounce from b to e is equal to $me/|u'_y| =$
 77 $\frac{1}{r}me/ac = \lambda^2/r$. More generally, δ is the ratio between the time spent on be and that
 78 spent on cb . By symmetry, the same ratio δ holds between the travel times along any two
 79 consecutive edges on the trajectory. This follows from the fact that the travel time along an
 80 edge is itself a ratio length/speed and that, from one boundary ∂P_k to the next, ∂P_{k+1} , the
 81 ratio between consecutive lengths is independent of k and the same is true of consecutive
 82 speeds. This implies a travel time of δ^k on ∂P_k . Convergence implies that $\delta < 1$, which,
 83 by (1), means that λ must be less than the smaller root of $\lambda^2 \cos \theta - 2\lambda + \cos \theta$ (since the
 84 larger one exceeds 1). This gives us the inequality $\lambda < (1 - \sin \theta)/\cos \theta$. Note that this
 85 condition is not implied by the previous requirement that $0 < \lambda < \cos \theta$. ◀

86 By (1), setting $r = \rho$ for any $\lambda < \cos \theta$ produces a valid particle system traveling inward
 87 through the (n, λ) -tiling. Of course, the interesting question is whether this holds for *any* value

88 of the coefficient of restitution. We address this issue below in the context of one-dimensional
89 systems.

90 2.4 One-dimensional collapse

91 The real parts of the $2n$ particles' positions in the unit disk \mathcal{D} describe a one-dimensional
92 particle system. To see why, it is useful to distinguish between the *positive* particles, those
93 numbered $1, \dots, n$ counterclockwise around \mathcal{D} , from the others, the *negative* particles. The
94 name comes from the fact that the positive (resp. negative) particles always remain in the
95 upper (resp. lower) complex halfplane. Each positive particle j is naturally paired with the
96 negative particle $2n + 1 - j$, since their trajectories are conjugate. Particles can only collide
97 with other particles of the same sign or with their conjugates; in the latter case, the collision
98 does not alter the motion along the real axis. All the other collisions occur in conjugate
99 pairs. This shows that the real-axis motion of the positive particles alone constitutes a bona
100 fide collision system over n particles with the same coefficient of restitution.

101 ► **Theorem 2.2.** *Fix any integer $n > 2$, and write $\theta = \pi/n$ and $r_0 = (1 - \sin \theta)/(1 + \sin \theta)$.
102 Given any positive coefficient of restitution $r \leq r_0$, there is a scaling factor λ such that
103 the line projection of the (n, λ) -tiling forms the trajectory of a one-dimensional n -particle
104 system exhibiting inelastic collapse. The collapse time is $r/(r - \lambda^2)$ for any $r < r_0$ and
105 $\lambda = q \cos \theta - (q^2 \cos^2 \theta - r)^{1/2}$, where $q = (1 + r)/2$.*

106 **Proof.** Setting $r = \rho$ in (1) yields the quadratic equation

$$107 \quad \lambda^2 - 2q(\cos \theta)\lambda + r = 0; \quad (2)$$

108 hence $\lambda = q \cos \theta \pm \sqrt{q^2 \cos^2 \theta - r}$. The roots need to be real; hence $\sin \theta \leq p/q$ or,
109 equivalently, $r \leq r_0$. We verify that $0 < \lambda < \cos \theta$, as required of a valid (n, λ) -tiling, which
110 is a consequence of $\sqrt{q^2 \cos^2 \theta - r} < p \cos \theta$. By Lemma 2.1, the collapse time is infinite if
111 $\delta = \lambda^2/r \geq 1$ and equal to $\sum_{k \geq 0} \delta^k = 1/(1 - \delta) = r/(r - \lambda^2)$ if $\delta < 1$. The smaller root
112 of (2), if strictly smaller, always satisfies the latter condition while the larger one never does.
113 This follows from the fact that $\lambda_- \lambda_+ = r$, $q \cos \theta \geq \sqrt{r}$, and $\lambda_+ \geq q \cos \theta$; hence $\lambda_+^2 \geq r$. ◀

114 In our construction, the upper bound on the coefficient of restitution is $(1 - \sin \theta)/(1 + \sin \theta)$.
115 As n goes to infinity, this gives us $n \gtrsim 2\pi/(1 - r)$, which matches the bounds from [1, 2].
116 For $n = 3$, our construction rediscovers the classic bound of $7 - 4\sqrt{3}$ [4, 6, 7].

117 3 Distinct Coefficients of Restitution

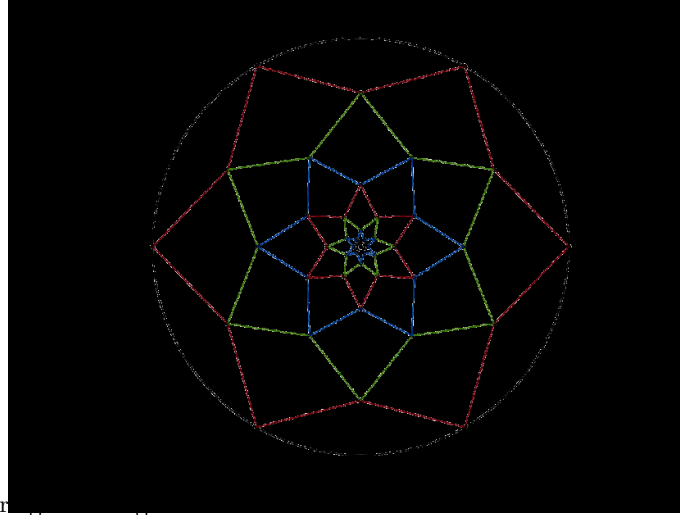
118 Our construction does not require a fixed scaling λ . Instead of placing the vertices on
119 circles of radius λ^k for $k \geq 0$, we can use an arbitrary decreasing radius sequence $(\lambda_k)_{k \geq 0}$,
120 with $\lambda_0 = 1$. We assign a coefficient restitution r_k for the collisions at radius λ_k ; the
121 dependency on k might reflect a gain or loss of elasticity after repeated collisions. For
122 notational convenience, let $p = (1 - r_1)/2$, $\lambda = \lambda_1$, and $\mu = \lambda_2$. By reference to Figure 3, we
123 now kick a particle from a to b with velocity $u = b - a$ (using complex numbers), and one
124 from c to b with velocity $v = b - c$. Post-collision, the first particle travels from b to d with
125 velocity $u' = pu + (1 - p)v = \sigma_1(d - b)$, for some $\sigma_1 > 0$; hence $b - c + p(c - a) = \sigma_1(d - b)$.
126 Since $a = 1$, $b = \lambda e^{i\theta}$, $c = e^{2i\theta}$, and $d = \mu$, we divide the equation by $e^{i\theta}$ and find that

$$127 \quad \lambda - e^{i\theta} + 2pi \sin \theta = \sigma_1(\mu e^{-i\theta} - \lambda);$$

128 therefore, $\lambda - \cos \theta = \sigma_1(\mu \cos \theta - \lambda)$ and $r_1 = \sigma_1 \mu$. More generally, for $k > 0$, we replace λ
 129 and μ by λ_k and λ_{k+1} , respectively, and we scale the relations by λ_{k-1} :

$$130 \quad \sigma_k = \frac{\lambda_{k-1} \cos \theta - \lambda_k}{\lambda_k - \lambda_{k+1} \cos \theta} \quad \text{and} \quad r_k = \frac{\cos \theta - \lambda_k / \lambda_{k-1}}{\lambda_k / \lambda_{k+1} - \cos \theta}. \quad (3)$$

131 Of course, we retrieve the relation $r = \rho$ in (1) in the case $\lambda_k = \lambda^k$ corresponding to having
 132 fixed coefficients of restitution.



133 ■ Figure 3 An intricate geometric diagram illustrating the concept of finite-time inelastic collapse.

134 3.1 Finite-time inelastic collapse

135 From the relation $u' = \sigma_1(d - b)$, we see that the time spent crossing bd is precisely $1/\sigma_1$.
 136 More generally, $1/\sigma_k$ is the time spent on the $(k + 1)$ -st star polygon, given a unit travel
 137 time on the previous polygon. It follows that the total travel duration is the sum of all the
 138 products of the form $1/\sigma_1 \cdots \sigma_k$, which is

$$139 \quad 1 + \sum_{k=1}^{\infty} \prod_{j=1}^k \frac{\lambda_j - \lambda_{j+1} \cos \theta}{\lambda_{j-1} \cos \theta - \lambda_j}. \quad (4)$$

140 By projection onto the real line, finite-time inelastic collapse is guaranteed if

$$141 \quad \lambda_{k+1} \geq \frac{1+c}{\cos \theta} \lambda_k - c \lambda_{k-1},$$

142 for some fixed $c < 1$. Again, we can check that, if $\lambda_k = \lambda^k$, then bounded travel time means
 143 that $\lambda < \frac{1}{\cos \theta} - \tan \theta$, as claimed in Lemma 2.1.

144 3.2 Red-blue particles

145 Consider two species of particles, blue and red. The blue particles collide together with the
 146 coefficient of restitution r_1 and the same is true of the red ones. Particles of different colors,
 147 however, collide with the coefficient r_2 . Arrange the particles as usual, with the sequence
 148 blue, blue, red, red, blue, blue, red, red, etc. Set the scaling factor $\lambda_k = \mu^j$ if $k = 2j$, and
 149 $\lambda_k = \lambda \mu^j$ if $k = 2j + 1$. By (3), we choose

$$150 \quad r_1 = \frac{\mu(\cos \theta - \lambda)}{\lambda - \mu \cos \theta} \quad \text{and} \quad r_2 = \frac{\lambda \cos \theta - \mu}{1 - \lambda \cos \theta}.$$

151 Each factor in (4) is of the form

$$152 \quad \frac{\lambda_j - \lambda_{j+1} \cos \theta}{\lambda_{j-1} \cos \theta - \lambda_j} = \begin{cases} \mu(1 - \lambda \cos \theta)/(\lambda \cos \theta - \mu) = \mu/r_2 & \text{if } j \text{ is even} \\ (\lambda - \mu \cos \theta)/(\cos \theta - \lambda) = \mu/r_1 & \text{else.} \end{cases}$$

153 The travel time is finite if $\mu^2 < r_1 r_2$, which is

$$154 \quad \mu(\lambda - \mu \cos \theta)(1 - \lambda \cos \theta) < (\cos \theta - \lambda)(\lambda \cos \theta - \mu).$$

155 ——— **References** ———

- 156 **1** D. Benedetto and E. Caglioti. The collapse phenomenon in one-dimensional inelastic point
157 particle systems. *Physica D: Nonlinear Phenomena*, 132(4):457 – 475, 1999.
- 158 **2** B. Bernu and R. Mazighi. One-dimensional bounce of inelastically colliding marbles on a
159 wall. *Journal of Physics A: Mathematical and General*, 23(24):5745 – 5754, 1990.
- 160 **3** B. Cipra, P. Dini, S. Kennedy, and A. Kolan. Stability of one-dimensional inelastic collision
161 sequences of four balls. *Physica D: Nonlinear Phenomena*, 125(3):183 – 200, 1999.
- 162 **4** P. Constantin, E. Grossman, and M. Mungan. Inelastic collisions of three particles on a line
163 as a two-dimensional billiard. *Physica D: Nonlinear Phenomena*, 83(4):409 – 420, 1995.
- 164 **5** S. McNamara. Inelastic collapse. pages 267 – 277, 2002.
- 165 **6** W.R. Young, S. McNamara. Inelastic collapse and clumping in a one-dimensional granular
166 medium. *Physics of Fluids A: Fluid Dynamics*, 4(3):496 – 504, 1992.
- 167 **7** K. Shida and T. Kawai. Cluster formation by inelastically colliding particles in one-
168 dimensional space. *Physica A: Statistical Mechanics and its Applications*, 162(1):145 –
169 160, 1989.
- 170 **8** L.P. Kadanoff, T. Zhou. Inelastic collapse of three particles. *Physical review E*, 54(1):623
171 – 628, 1996.